UNIVERSIDAD TÉCNICA FEDERICO SANTA MARÍA

DEPARTAMENTO DE FÍSICA

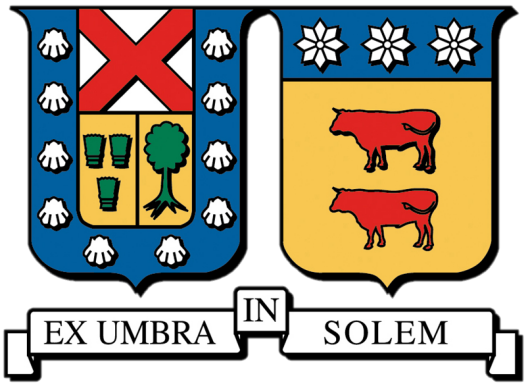

Galaxy Morphologies in CHANCES Galaxy Survey

Javiera Vivanco Robles

MEMORIA PARA OPTAR AL TÍTULO DE LA LICENCIATURA EN ASTROFÍSICA

Tutor: Yara Jaffé Ribbi

Co-tutor: Diego Pallero Astargo

December 20, 2024

Abstract

This thesis investigates galaxy classification and its relation to the local and global environment by using publicly available Galaxy Zoo DESI classifications, which combine citizen science and deep learning, and CAS measurements, to classify the galaxies in the CHANCES target selection catalog, which includes galaxies from over 50 clusters, extending out to out to $5R_{200}$. We aim to determine which classification method performs better for different morphological types and then analyze the morphology-density and morphology-radius relations. To accomplish this, we defined a threshold for the vote fractions through visual inspection to classify galaxies into morphology types, and used public optical imaging to measure the CAS parameters. This led to the classification of 43.885 galaxies by deep learning, with many galaxies excluded due to issues like shredding and filter constraints. Deep learning performed better at identifying mergers and edge-on disks, which have distinctive appearances. Using CAS, we classified only 11.321 galaxies, as the strict parameter boundaries and poor measurement quality caused by incomplete image processing limited the classification. CAS performed best for classifying elliptical and disk galaxies. The morphology-density and morphology-radius relations revealed that the fraction of elliptical galaxies increases with higher densities and shorter radii, with their morphology primarily influenced by local density. In contrast, disk galaxies increase with larger radii and decrease with higher densities, with environmental effects dominating inside the cluster radius. Mergers are more likely to occur outside the virial radius and at higher densities, suggesting that other physical mechanisms are causing morphological changes within the cluster. To enhance this work, future studies will incorporate the lenticular morphology and improve the overall classification process by addressing overlooked aspects.

Acknowledgement

I would like to extend my gratitude to my supervisors, Dr. Yara Jaffé and Dr. Diego Pallero, for their constant support throughout my thesis journey. Your kindness, immense knowledge, and passion for teaching have been truly inspiring. Your courses, work ethic, and dedication are part of what revived my enthusiasm for astronomy and motivated me to pursue a future in academia. Thank you for continually encouraging me and helping me believe in myself more. With your guidance, this process has been an enjoyable and fulfilling experience, far beyond what I initially feared.

I would also like to thank the rest of the extragalactic group for their contributions to the development and writing of my thesis. I appreciate your willingness to help.

My sincere thanks also goes to Dr. Matthias Schreiber for allowing me to be his research assistant, which enabled me to gain valuable knowledge and my first experience in the world of academia.

I thank everyone who supported me in different ways throughout my studies, especially when I decided to change my career path. I appreciate your support, companionship, and laughter.

I am deeply thankful to my family for their support and constant reminder of their belief in me and my abilities. I especially want to thank my mom; I truly value the sacrifices and great effort she has made, which have allowed me to focus on my studies and complete them without worries. Thank you for telling me that I can achieve great things.

Lastly, a heartfelt thanks to Evelyn for her immense love and continuous support. Thank you for also helping me with some of the little yet important things for my thesis. I admire you greatly, and you inspire me every day. Thank you for always being there for me, for encouraging me and motivating me to build a bright future.

Sincerely, Javiera Vivanco.

Contents

Chapter 1

Introduction

Galaxies are among the most fundamental structures in the universe, revealing the processes that shape its large-scale structure and evolution. By studying them, astronomers gain a better understanding of the distribution of matter, the influence of gravity, and the role of dark matter. Galaxies are not distributed uniformly; instead, they cluster together to form massive structures such as clusters and superclusters, connected by vast filaments of dark matter (Bond et al., 1996). These structures provide insight into how matter has evolved over cosmic time.

In order to understand the overall evolution of the universe, it is important to study the evolution of galaxies. Over time, galaxies experience significant transformations due to various factors, such as gas accretion, mergers, and internal changes, including star-formation rate, age, and the dynamics of their components. Therefore, as galaxies evolve, their morphological characteristics change, reflecting their properties and dynamic history. Galaxies are broadly categorized into several morphological types, a classification that dates back to the work of Edwin Hubble, who created the Hubble sequence (Hubble, 1926). He separated galaxies into ellipticals, smooth and featureless galaxies with an ellipsoidal shape; spirals, characterized by well-defined arms winding out from a central bulge; barred spirals, similar to spirals but with a prominent bar structure across the center; and lenticulars, disk-shaped galaxies lacking prominent arms. This sequence has since been modified to include additional types, such as irregular galaxies, with chaotic, non-symmetrical structures.

The morphology of galaxies it is tighly correlated with the environment in which they are located. This has been extensively studied, particularly the morphology-density relation. Dressler (1980) examined 55 galaxy clusters and found that the fraction of elliptical galaxies increases in denser environments, while spiral galaxies dominate in less dense regions. Additionally, Goto et al. (2003) compared the morphology-density relation for galaxies at a redshift $0.01 < z < 0.054$ with galaxies at $z \sim 0.5$, finding that these relationships remain consistent over time, which indicates that the morphology-density relation is not a recent phenomenon. However, Whitmore

et al. (1993) argued that the morphology-radius relation is stronger than the morphology-density relation based on his analysis of the same 55 clusters studied by Dressler (1980), finding that the elliptical galaxies are more prominent at the centers of clusters, while spiral galaxies are nearly absent in these regions. The study of both relationships raises questions about how galaxies form and which mechanisms – local or global – are more responsible for determining their morphology.

Some of the proposed local physical mechanisms to explain the different morphologies are: (i) ram pressure stripping of gas (Gunn and Gott, 1972), which occurs when galaxies fall into clusters and experience strong pressure from the surrounding medium, causing the gas in the galaxy to be stripped away, (ii) merging of galaxies, a process where two galaxies interact sufficiently to merge into one, potentially leading to the formation of elliptical galaxies (Mamon, 1992), (iii) galaxy harassment, involving high-speed impulsive encounters between galaxies within a cluster, which can alter the morphology of the interacting galaxies (Moore et al., 1996). On the other hand, some proposed global physical mechanisms include: (i) the tidal force exerted by the entire galaxy cluster, which are strong enough to cause significant changes or activity in the spiral galaxies within the cluster (Byrd and Valtonen, 1990), (ii) changes in the rate of infalling galaxies into clusters, which lead to SFR truncation in cluster galaxies, resulting in changes to their color (Kodama and Bower, 2001). Domínguez et al. (2001) found that global mechanisms dominate in high-density environments, with the cluster mass density being a primary parameter for segregating morphology types, while local density prevails in the outskirts, where the overall influence of the cluster is relatively minor compared to local effects. However, there is still no definitive answer as to which mechanisms are responsible for the evolution of galaxies in different locations of the cosmic web.

A critical step in addressing this question is the accurate classification of galaxies. This task is challenging due to the vast diversity in galaxy structures, the effects of projection, limitations in data resolution, and the various modes of galaxy evolution. Historically, visual inspection has been the primary method for categorizing galaxy morphology, with the Hubble morphological system (Hubble, 1926) being the most widely used. It is useful to determine global morphological parameters such as diskyness, the presence of barred arms, etc. However, it becomes impractical for classifying large volumes of galaxies, especially with the continuous flow of new data. This has led to the adoption of machine learning (ML) models and Deep Learning (DL) techniques for galaxy classification. ML algorithms are able to classify galaxies using features extracted from photometric or/and spectroscopic data, relying on labeled datasets, i.e, galaxies that have already been classified (e.g. Vavilova, I. B. et al. (2021)). This is much faster and consistent than human classification, although the performance is highly dependent on the quality of the training dataset. DL has revolutionized galaxy classification by enabling models to learn directly from raw images. A notable example of this is Galaxy Zoo (Walmsley et al., 2023), a project that combines

citizen science through visual inspection with DL. Here, DL algorithms are trained using the vote fractions from citizens about the morphology of a large number of galaxies, allowing the model to predict the votes for other galaxies that have not been inspected by humans. Other methods of morphology classification include parametric techniques, which provide a quantitative alternative by fitting observed galaxy properties, allowing for the determination of structural parameters such as the Sérsic index (Sérsic, 1963) or performing bulge-disk decompositions to separate a galaxy's components. Unfortunately, these methods are limited by the complexity of galaxy structures, which predefined models may overlook. There are also non-parametric methods that derive parameters directly from the observed data without relying on models. Among these is the CAS system (Conselice, 2003), a method that measures three properties: the concentration of light (Concentration), the asymmetry in the galaxy's structure (Asymmetry), and the smoothness of the light distribution (Smoothness). Additional non-parametric approaches include the Gini coefficient, which quantifies the relative distribution of pixel flux values, and M20, which represents the second-order moment of the brightest 20% of the galaxy's flux (Lotz et al., 2004). In this case, high-resolution, uncontaminated imaging is required, which makes it even more challenging to apply to distant galaxies.

Despite significant progress in this field, there are still unaswered questions, particularly regarding the mechanisms that drive changes in galaxy morphologies and how to effectively classify them. In this work, we aim to study the morphology-density and morphology-radius relations using data from the CHANCES (CHileAN Cluster galaxy Evolution Survey) project. CHANCES is a 4MOST community survey designed to study the formation and evolution of galaxies with a particular focus on their environments through multi-object spectroscopy (Sifón et al., 2024). For this study, we use Galaxy Zoo DESI catalog and derive CAS parameters using public optical imaging for morphology classification. In addition, we use the CHANCES target selection for the environment analysis, which contain photometric members of over 50 clusters, out to 5 virial radius. Additionally, we aim to discuss the effectiveness of these techniques for galaxy classification and the challenges they may present. This thesis is organized as follows: In chapter 2 we describe the data from the CHANCES target selection and the Galaxy Zoo DESI catalogs. In chapter 3 we explain in detail the galaxy classifications and the measurements of local galaxy density. In chapter 4 we present our results from the classifications, as well as the morphology-density and morphology-radius relations, followed by a discussion. In section 5 we summarize our project and offer suggestions for future research.

Chapter 2

Data

2.1 CHANCES

We use the galaxy catalogue built as part of the target selection process for the CHANCES (CHileAN Cluster galaxy Evolution Survey) 4MOST spectroscopic survey, designed to study the formation and evolution of galaxies, which is set to begin in 2025 (Sifón et al., 2024). The catalog used is the CHANCES Low-z sub-survey, targeting 50 clusters at $z \leq 0.07$. The galaxies were selected to be photometric members of these massive clusters, extending out to $5R_{200}$, as well as 2 large supercluster regions. Selection criteria included $r < 20.5$ magnitudes and photometric redshifts consistent with their host cluster's redshift. This catalog contains a total of 126.452 galaxies. However, for this work, we focus only on the galaxies within clusters and exclude those in superclusters, since we aim to study the morphology-radius relation, and defining the center of a supercluster is harder due to its non-spherical nature. Considering only these galaxies, we have 77.188 galaxies.

2.2 Galaxy Zoo DESI

Walmsley et al. (2023) presents the Galaxy Zoo DESI catalog, which provides detailed morphological information for 8.67 million galaxies within the DESI Legacy Survey. Using deep learning models trained on volunteer input from Galaxy Zoo, the catalog provides predicted fractional responses to various questions about galaxy morphology, rather than discrete classifications. The DESI-LS data release is composed by four individual surveys: DECaLS, BASS, MzLS, and DECam, which together cover a sky area of $19.437\,\mathrm{deg}^2$, shown in Figure 2.1. The catalog includes galaxies with magnitude $r < 19$ and surface brigthness $\mu > 18$ mag arcsec^{-2}, criteria chosen by the authors to exclude dim sources and minimize stellar contamination.

2.3 Catalogue matching

We match the CHANCES and Galaxy Zoo catalogs by their right ascension and declination coordinates using TOPCAT, allowing for a maximum positional error of 1.0 arcseconds. For this matching process, we focus exclusively on the galaxies within clusters in the CHANCES catalog, excluding those in superclusters, as previously mentioned. This match results in 47.582 galaxies in common, corresponding to 61.64% of the CHANCES catalog. In Figure 2.1, we can see that some galaxies do not match because they are located in areas not covered by the GZ catalog. However, many unmatched galaxies are in regions where matches do exist, and one reason for this discrepancy is shredding. There were multiple sources detected from a single galaxy, mistakenly classifying them as different objects. This is illustrated in the Figure 2.2, where red dots represent "galaxies" that did not match, while blue dots indicate successful matches.

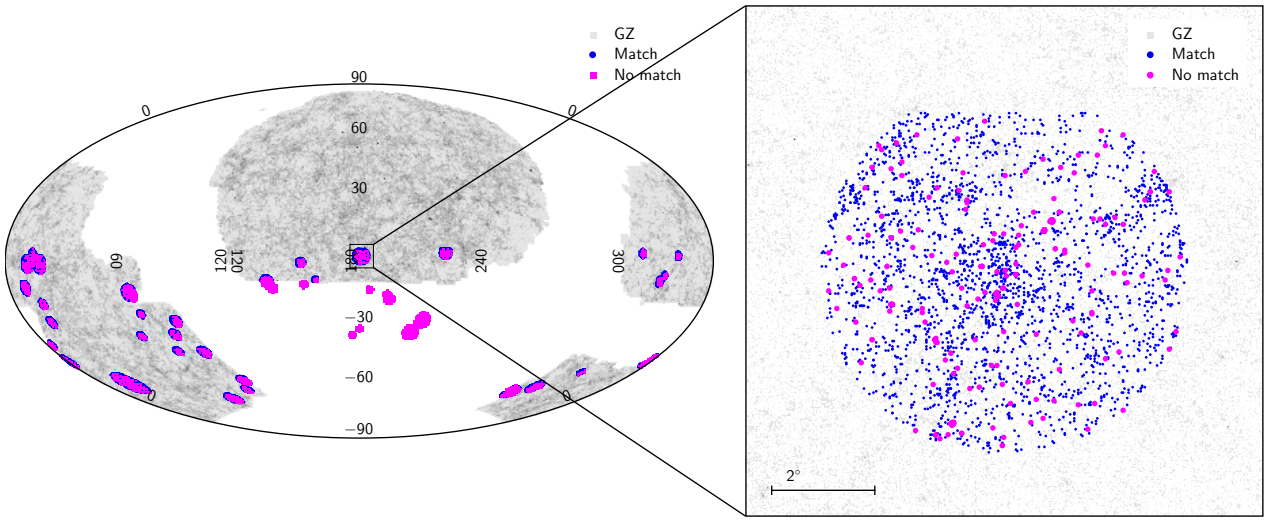

Figure 2.1: Sky coverage of the Galaxy Zoo (GZ) DESI and CHANCES catalogs, highlighting matched and unmatched galaxies between them. The right panel shows a zoomed-in region in the cluster MKW 4, as an example, for better visualization.

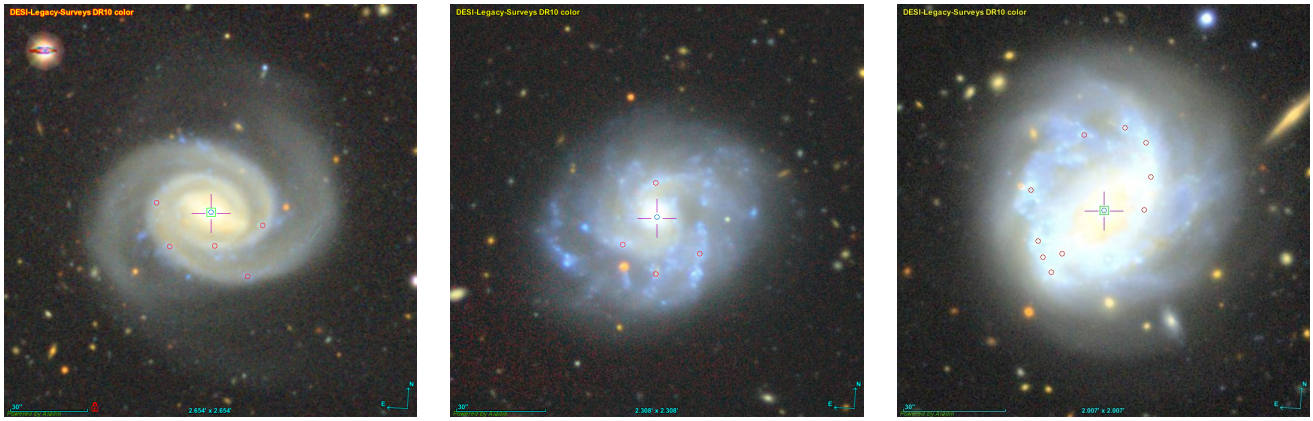

Figure 2.2: Examples of shredding in the CHANCES catalog, shown in optical color from DESI Legacy Survey DR10 images in Aladin. Red dots are unmatched "galaxies" and blue dots are matched galaxies.

To address this issue within the CHANCES target selection catalog, and help clean it, we cross-matched it with the Tractor table from the Legacy Survey DR8 database using the X-Match service provided by Astro Data Lab (https://datalab.noirlab.edu/xmatch.php). A maximum radius of 0.5 arcseconds was used for the crossmatch. This process allowed us to obtain the fraction of the model in de Vaucouleurs (`fracdev`), the half-light radius of the de Vaucouleurs model (`shapedev_r`), and the half-light radius of the exponential model (`shapeexp_r`). Using these parameters, the radius of each galaxy was computed based on the equation presented in Walmsley et al. (2023):

$$r = \text{fracdev} \cdot \text{shapedev\_r} + (1 - \text{fracdev}) \cdot \text{shapeexp\_r}. \tag{2.1}$$

During this process, we observed that some sources had null or zero values for their radii. While this corresponded to non-galaxy sources, we also found cases where actual galaxies shared these characteristics, meaning we could not simply remove all sources with these radii. Therefore, to systematically filter out misclassified sources, we defined a search radius of 0.02 degrees around each source. If more than two sources with a null or zero value for their radii were found within this radius, the region was flagged as a possible shredding case. This radius was chosen to detect shredding cases without including too many closely spaced galaxies. From this, we obtained a preliminary list of approximately 5.500 sources.

Using the Aladin tool, we visually inspected all flagged cases to exclude actual galaxies mistakenly included in the list. This step revealed a significant number of closely located galaxies, especially in dense regions such as the Shapley supercluster. After this review, the list was reduced to approximately 1.590 sources, containing only actual shredding cases.

For the remaining cases, all sources within 0.03 degrees of each other were grouped together

as belonging to the same galaxy. In each group, the brightest source was designated as the actual galaxy. Galaxies with larger radii required further inspection. For these cases, we grouped sources iteratively, ensuring that the brightest source of the previously brightest sources was identified as the actual galaxy. This resulted in 220 galaxies. There were also 14 galaxies whose central coordinates were not part of the CHANCES catalog, but which had detected sources within the galaxy. In these cases, we added the actual coordinates to the catalog and removed all the other sources. In total, there were 234 galaxies with shredding.

Since there are only 1.590 sources related to cases of shredding, this cannot be the sole reason why only 61.64% of the CHANCES catalog matches with Galaxy Zoo DESI. As previously mentioned, one of the filters used by the GZ authors is $\mu > 18$, which was calculated using $\mu = \text{mag}_r + 2.5 \log_{10}(\pi r^2)$ (Walmsley et al., 2023). Therefore, sources with a radius of zero or null have an undefined or null surface brightness. In fact, 97% of the galaxies that do not match have this undefined brightness. The reason why the remaining 3% of galaxies do not match remains unknown. Upon visual inspection of many of these galaxies, we noticed that they could be easily assigned a classification. Thus, a potential future step could involve performing transfer learning with the deep learning model used by GZ, Zoobot[1], which is publicly available. This approach would allow us to obtain vote fraction predictions for each answer for our own galaxies, without the need for them to be part of an external catalog.

[1] https://github.com/mwalmsley/zoobot

Chapter 3

Methods

3.1 Classification of galaxies using vote fractions

We use the vote fractions from the GZ DESI catalog to determine the morphology of each galaxy, between early-type, late-type, edge-on disk and merger. While there are several columns of vote fractions corresponding to different responses for various questions, our focus is on the vote fractions related to three specific questions:

1. "Is the galaxy simply smooth and rounded, with no signs of a disk?" with answers "Smooth" "Features or disk" and "Artifact".

2. "Could this be a disk viewed edge-on?" with answers "Yes" and "No".

3. "Is the galaxy merging and disturbed?" with responses "Merging", "Major disturbance", "Minor disturbance", and "None".

This works as the following example: if the vote fraction for the answer "Smooth" to the first question is 0.90 for a given galaxy, it means that 90% of the predicted responses suggest that the galaxy is smooth, and therefore early-type. However, this arises the question of how to determine an appropriate threshold for classification. If we set a threshold of, for example, 0.80, we will classify galaxies for which we have high confidence in their morphological classification, but this may result in many unclassified galaxies, wasting significant data from the catalogs.

To address this, we defined a threshold through visual inspection. We created four large mosaics of images, one for each of the answers "Smooth", "Features or disk", "Edge-on disk", and "Merging". Each mosaic is composed of different galaxies, sorted by their vote fractions for the respective answers, using one random galaxy for each vote. This results in approximately 90 images per mosaic, except for the "Edge-on Disk" mosaic, which includes 10 images. These are presented

in Fig. A.1, A.2, A.3 and A.4, for the answers "Smooth", "Features or disk", "Edge-on disk" and "Merger", respectively. With this approach, we aimed to identify the vote fraction at which galaxies begin to exhibit the desired morphology. For the "Features and disk", "Smooth", and "Edge-on disk" vote fractions, we observed that galaxies of each morphology starts to appear more clearly at a vote fraction of 0.5, with galaxies at higher vote fractions also displaying such morphology. For the "Merger" vote fractions, the threshold is 0.45. However, to maintain consistency in the analysis, we decided to set a uniform threshold of 0.5 for these four morphologies[1]. It is worth noting that, for elliptical and disk galaxies, there is some contamination in the sample due to the presence of intermediate galaxies at lower vote fractions (lower confidence levels). In future studies, we aim to perform more rigorous classifications.

After defining the threshold as 0.5, we classified the galaxies such that they must have a vote fraction greater than or equal to 0.5 for the respective morphology. Additionally, to distinguish between classifications, a galaxy must have a vote fraction for "Merger" less than 0.5 to be classified as something other than a Merger. Similarly, for a galaxy to be classified as late-type, its vote fraction for "Edge-on disk" must also be less than 0.5. These conditions or cuts are presented in Table 3.1, along with the number of galaxies classified under each morphology. 92.23% of the total of galaxies in the matched catalog were successfully classified. The remaining galaxies were not classified because they either have high vote fractions for "Artifact" or had low vote fractions for both 'Smooth' and 'Features and Disk,' leaving them without a distinguishable morphology.

Morphology	Cut	Number of galaxies
Early-type	`smooth` ≥ 0.5 `merger` < 0.5	29.225
Late-type	`features or disk` ≥ 0.5 `merger` < 0.5 `disk edge-on` < 0.5	10.833
Edge-on	`disk edge-on` ≥ 0.5 `merger` < 0.5	3.225
Merger	`merger` ≥ 0.5	602

Table 3.1: Cuts used for the morphology classification of galaxies in the CHANCES catalog, along with the number of galaxies in each category, based on visual inspection by the authors, as explained in Section 3.1.

[1]This criteria was defined in agreement between four astronomers: Yara Jaffé, Diego Pallero, Diego Correa, and Javiera Vivanco.

3.2 CAS parameters measurement

We used the Python package `statmorph` (Rodriguez-Gomez et al., 2019) to measure the CAS parameters for each galaxy of the matched catalog, as this allows a comparison with the classification based on vote fractions predicted by GZ (deep learning). This code derives the concentration (C) of light, the asymmetry (A) in the galaxy's structure, and the smoothness (S) of the light distribution (Conselice, 2003), along with other parameters such as Gini-M20 (Lotz et al., 2004), MID statistics (Multimode, Intensity, Deviation) (Freeman et al., 2013), Sérsic index, etc. In this work we will only use the CAS parameters.

This code requires as input an optical image in FITS format with background subtraction applied, along with a segmentation map of the source. The optical images we used are from the Legacy Survey DR10, taken in the r band, with a pixel scale of 0.1 arcseconds and a size of 240x240 pixels. The background was subtracted using the `photutils` package (Bradley et al., 2024). A 2D median background estimator with a sigma-clipping threshold of 3.0 was applied, and the background was estimated over a 50x50 pixel grid. This background was then subtracted from each pixel of the original image. With the same library, a Gaussian kernel was created with a standard deviation of 3.0 and a size of 5x5 pixels. This kernel was used as the Point Spread Function (PSF), and was convolved with the background-subtracted data using `astropy` to improve the resolution by smoothing it. The segmentation map was generated using the `photutils` package by calculating a detection threshold based on the background noise of the image. Then, the convolved image was then analyzed to detect sources that exceeded this threshold. Using this map, we identified the main source by selecting the one with the largest area and masked other sources around the galaxy present in the image. An example of the whole process is presented in Figure 3.1, where the steps are illustrated sequentially from left to right. The last two images, located in the middle and right positions of the bottom row, serve as the input for `statmorph`. The results of the parameter measurements for this example are shown in Figure 3.2, which was generated using the `make_figure` function from `statmorph`.

The code returns two flags that reports the quality of the fitted results for each galaxy: one for the morphology measurements (`flag`) and one for the Sersic fit (`flag_sersic`). A value of 0 corresponds to a good fit, 1 to suspicious, 2 to bad, and 3 to catastrophic. Before classifying the galaxies, we retain only those with `flag` ≤ 1, resulting in 37.489 galaxies out of 47.583. We classified these galaxies into six morphology types: ellipticals, early-disk, late-disk, edge-on, dwarf ellipticals and mergers. This classification was based on the criteria for each CAS parameter in the R-band presented in Table 6 of Conselice (2003), but using 2σ for ellipticals and 1.2σ for late-disks instead of 1σ, while keeping 1σ for early-disks, edge-ons, and dwarf ellipticals to reduce overlaps with other types. The number of deviations was selected to classify more elliptical and late-disk

galaxies and to achieve a more balanced sample. Additionally, mergers were classified using the conditions $A > 0.35 \wedge A > S$, following Conselice (2003). It is worth noting that `statmorph` uses the equation from Lotz et al. (2004) to compute the S parameter, but the original definition by Conselice (2003) includes an additional factor of 10. Therefore, we applied this factor to all S values to align with the mentioned criteria. The range of values used for each morphology and the number of galaxies classified are listed in Table 3.2. In this case, we classified 11.321 galaxies of the 37.489 galaxies with `flag` ≤ 1. Some reasons for the low number of classified galaxies will be discussed in Section 4.1. However, we believe that a primary factor is the strict parameter boundaries used in the classification process, which can be seen as a "box" for each morphology type. If a galaxy falls even slightly outside these boxes, it is not classified. To address this limitation in future studies, we propose a supervised machine learning approach that combines visual classification with CAS parameter measurements. This would likely result in fewer galaxies being left unclassified.

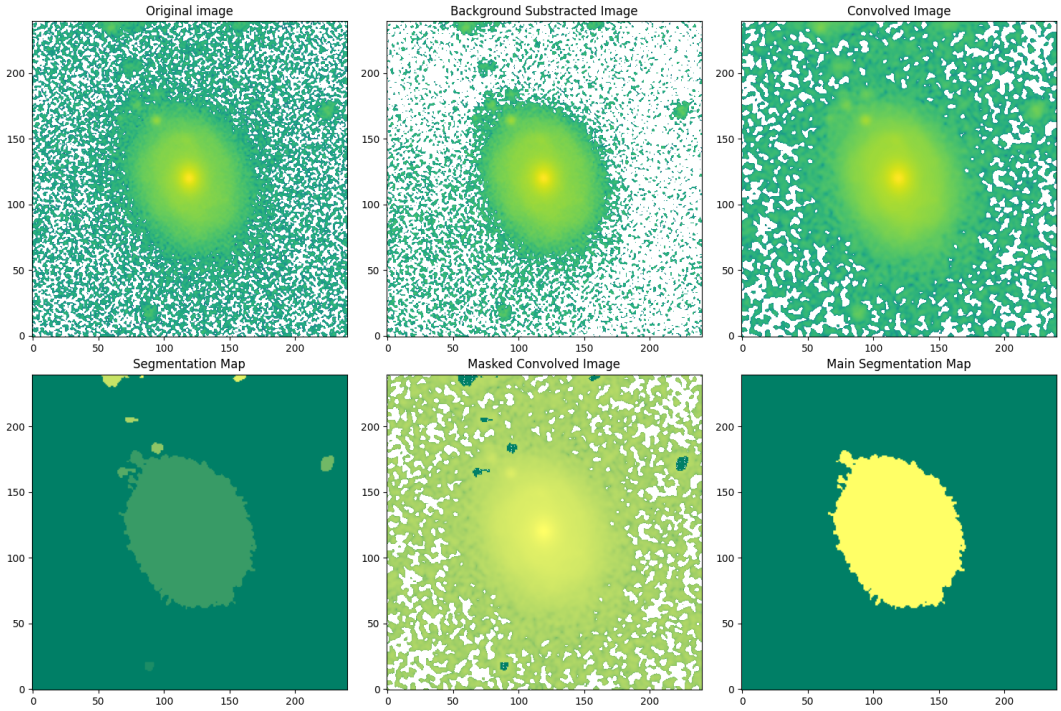

Figure 3.1: Example of the galaxy with coordinates RA: 0.4681 and Dec: -37.3962, illustrating the steps the original FITS file undergoes to produce the inputs for `statmorph`, which correspond to the final two images. The images are displayed on a logarithmic scale to make the differences more noticeable. This procedure is described in Section 3.2.

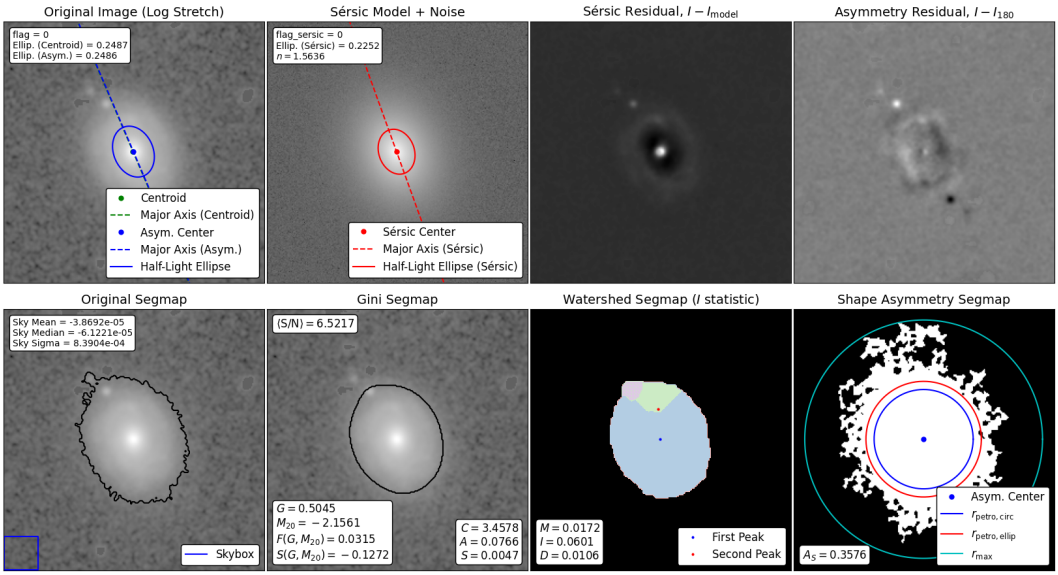

Figure 3.2: Example of the `statmorph` results for the galaxy with coordinates RA: 0.4681 and Dec: -37.3962. These figures are produced by the code's `make_figure` function, summarizing different morphological parameters. The two upper left panels include the best-fit elliptical and Sérsic models. The two upper right panels display the residual maps using the Sérsic model and a rotated image. The two bottom left panels show the input segmentation map and the generated Gini segmentation map. The two bottom right panels display the watershed segmentation map, where each color corresponds to a local brightness maximum, and the shape asymmetry segmentation map, which calculates Petrosian radii.

Morphology	C	A	S	Number of galaxies
Elliptical	4.4 ± 0.6	0.02 ± 0.04	0.00 ± 0.08	72
Early-disk	3.9 ± 0.5	0.07 ± 0.04	0.08 ± 0.08	484
Late-disk	3.1 ± 0.48	0.15 ± 0.072	0.29 ± 0.156	3.485
Edge-on	3.7 ± 0.6	0.17 ± 0.11	0.45 ± 0.20	448
Dwarf elliptical	2.5 ± 0.5	0.02 ± 0.03	0.00 ± 0.06	4.135
Merger	-	> 0.35	$< A$	2.697

Table 3.2: Range of values for each CAS parameter used to classify galaxies, based on Table 6 presented in Conselice (2003).

3.3 Characterization of enviroment

We characterize the local and global environment of galaxies through galaxy density and distance from the center of the cluster, respectively.

The local galaxy densities are derived from the work of Piraino-Cerda et al. (in prep.). They used the Voronoi Tessellation (VT) technique, a flexible method that does not assume a fixed aperture and automatically adjusts densities. VT creates polygonal cells around each point, allowing the calculation of local density by taking the inverse of each cell's area. They used the Voronoi function from Python's `scipy.spatial` module, which outputs the vertices of each polygon. The edges of the polygons were measured using the `separation` tool from Astropy. The area of each polygon was then calculated using the N-Triangulation method, with the galaxy's position as the center. For the area of each triangle, since the edges were determined using `separation`, which applies a non-Euclidean metric, the triangles were treated as spherical.

To calculate the distance of each galaxy to its respective cluster, we used the coordinates of each galaxy and the coordinates of the cluster center. For this, we applied the `separation` function from Astropy. The resulting angular distance in degrees was then converted into a physical distance in Mpc using the cosmological relation, taking into account the cluster's redshift, and the ΛCDM model with a Hubble constant (H_0) of 70 km/s/Mpc, a matter density parameter (Ω_{matter}) of 0.3, and a dark energy density parameter (Ω_λ) of 0.7.

Chapter 4

Results

4.1 Comparison between Galaxy Zoo (deep learning) and CAS morphologies

4.1.1 Ellipticals and disk-galaxies

Given that colour is known to tightly correlate with morphology, we compare the classifications made by deep learning and CAS. This is shown in Figure 4.1.

It is known that early-type galaxies are tipically red, while spiral/disk galaxies are bluer. However, from the CMD generated using Galaxy Zoo/Deep Learning, we note that many early-type galaxies appear to have bluer colors, and some spiral galaxies exhibit redder colors than expected. In contrast, the CMD generated using CAS provides more consistent results. Here, elliptical galaxies are red, forming a red sequence as expected, while dwarf galaxies also appear predominantly red, though a significant amount has bluer colors. Late-disk galaxies show a high density in the blue region, consistent with their ongoing star formation. Early-disk galaxies, however, are mostly red.

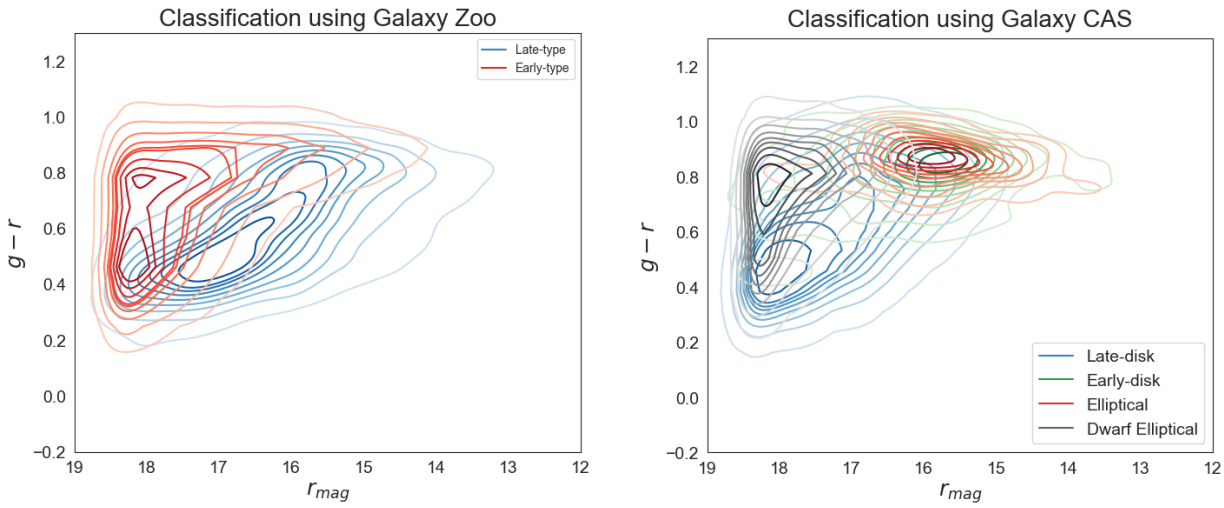

Figure 4.1: Color-Magnitude Diagram for $g - r$ color and r-band magnitude. The left panel shows late-type (blue contours) and early-type (red contours), classified based on vote fractions predicted by deep learning. The right panel shows late-disk (blue contours), early-disk (green contours), elliptical (red contours) and dwarf elliptical (grey contours) galaxies, classified using the CAS system.

To test if the deep learning morphologies could be improved, we imposed a stricter classification criteria, using a higher threshold for vote fractions. Using a threshold of 0.8 (instead of the original 0.5) did not lead to any improvement. This new CMD, shown in Figure 4.2, still shows a similar pattern as before, with many early-type galaxies appearing blue.

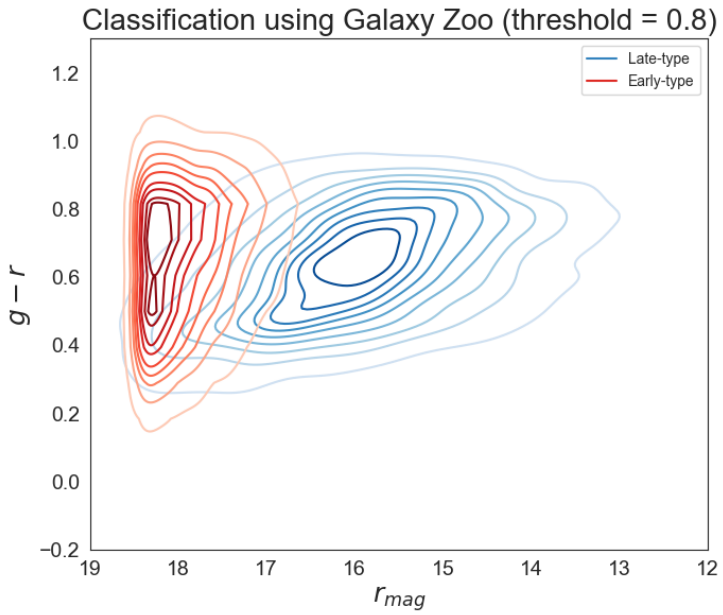

Figure 4.2: Color-Magnitude Diagram for $g - r$ color and r-band magnitude. It shows late-type (blue contours) and early-type (red contours), classified based on vote fractions predicted by deep learning, considering a threshold of 0.8.

We speculate that the inability for the deep learning method to adequatly classify these galaxies is due to the presence of many low-resolution galaxies that could be spirals or disk galaxies. Since their structures are unresolved, they appear featureless. Consequently, the deep learning model interprets these blurry galaxies as smooth and predicts high vote fractions for them, leading to a significant number of blue early-type galaxies in the classification. This bias arises because the model was trained on data labeled by volunteers from the Galaxy Zoo projects, who were often unable to discern the structures of such galaxies because of the low resolution (Cabrera-Vives et al., 2018). This has recently been studied by Medina-Rosales et al. (2024), who presented a method to obtain a de-biased model even when training on biased data. Examples of blue galaxies classified as early-type from our work are shown in Figure 4.3, alongside red galaxies also classified as early-type. It is evident that the image quality of the blue galaxies is poor, preventing the observation of their structures.

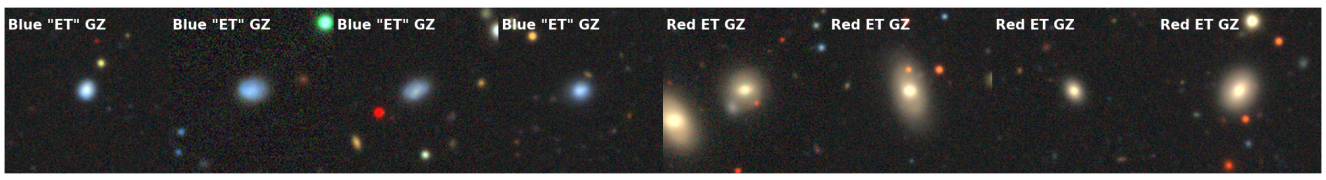

Figure 4.3: Random sample of galaxies classified as "Early-type" (ET) using Galaxy Zoo (GZ). The first four images show blue galaxies, while the last four show red galaxies.

A similar issue happens when classifying dwarf ellipticals using CAS, as it heavily depends on high imaging resolution; many low-resolution galaxies with bluer colors or disk-like features are misclassified as dwarf ellipticals. Besides the poor resolution of the images, we believe this issue may also arise because the FITS images from the Legacy Survey were all downloaded with the same pixel scale of 0.1. As a result, galaxies with smaller angular sizes appear very small in the images. We hypothesize that using an appropriate pixel scale for each galaxy's FITS image could improve the resolution, even slightly, and allow CAS to better compute features like clumpiness and asymmetry. To test this briefly, we recalibrated the pixel scale for a blue galaxy that was initially classified as a dwarf elliptical. Originally, its parameters were: $C = 2.261$, $A = 0.037$ and $S = 0.000$, and after adjusting the pixel scale, the parameters changed to $C = 2.579$, $A = 0.110$, $S = 0.055$. With these values updated, this galaxy would be classified as a late-disk galaxy instead of a dwarf elliptical. This is a preliminary demonstration that CAS, when using a more appropriate pixel scale for low-resolution galaxies, can classify them more accurately. Galaxy Zoo cannot improve by doing this, as it already uses images scaled according to the radius of each galaxy. Despite this problem, an advantage of CAS is its ability to distinguish between ellipticals and dwarf ellipticals. While dwarf ellipticals may not be classified as well, ellipticals are accurately identified.

Furthermore, CAS allows for a better distinction between early-disk (Sab) and late-disk (Scd) galaxies, which is crucial for detailed morphological studies. However, the excess of red early-disk galaxies may be due to lenticular galaxies being classified as early-disk. Additionally, these galaxies, along with others, may have been misclassified or not classified at all because we did not remove all the contaminating features in the images. While we eliminated features around the galaxy, we did not address those superimposed on the galaxy itself, which affects the model and, consequently, the values obtained for the parameters. Despite these caveats, for the reasons discussed, we conclude that CAS is more effective in classifying elliptical and disk galaxies in this context.

4.1.2 Edge-on and mergers

We further checked visually the deep learning and CAS classifications of peculiar galaxies such as edge-on disks and galaxy-galaxy mergers (see Figures 4.4 and 4.5). From this analysis, we observed that edge-on galaxies are best classified by Galaxy Zoo, although CAS also performs reasonably well in this category. However, CAS shows some contamination[1]. Additionally, Galaxy Zoo classifies significantly more galaxies as edge-on compared to CAS.

[1]In this work, we did not compute the completeness and contamination of each morphological type but aim to do so in future studies.

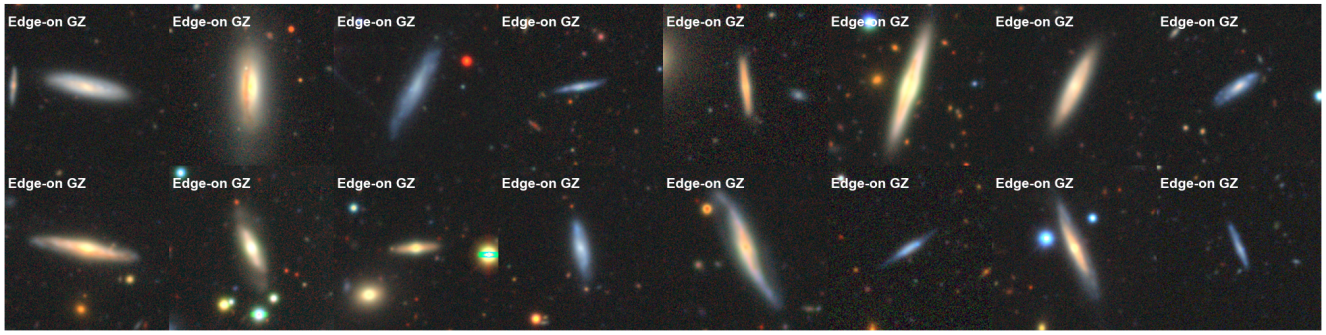

Figure 4.4: Random sample of galaxies classified as "Edge-on" using Galaxy Zoo (GZ).

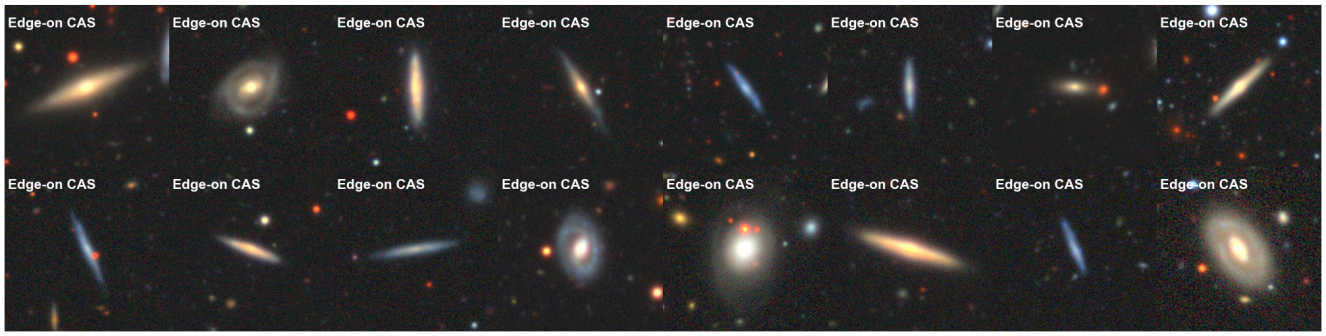

Figure 4.5: Random sample of galaxies classified as "Edge-on" using CAS.

On the other hand, CAS performs poorly in identifying merger galaxies, misclassifying non-mergers as mergers. This is evident in Figure 4.6, where most galaxies in the random sample are not mergers at all. In contrast, Galaxy Zoo performs this task very well, as seen in Figure 4.7, where actual merging galaxies are clearly identified. Actually, the deep learning model from Galaxy Zoo approaches the theoretical maximum agreement with the observed vote fractions for edge-on disk and merger classifications (Walmsley et al., 2023), i.e, the model is performing nearly as well as possible in classifying galaxies into these categories. This indicates that the model has learned to effectively identify the key features that distinguish edge-on and merger galaxies, demonstrating good accuracy in these classifications.

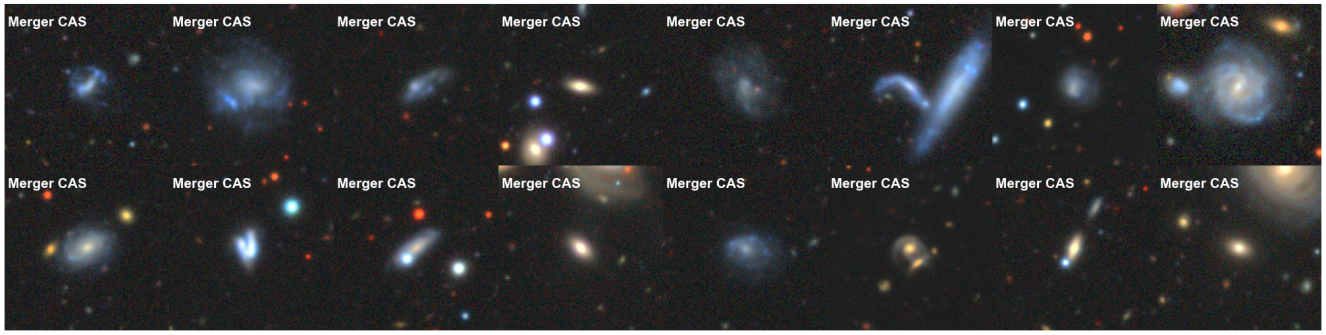

Figure 4.6: Random sample of galaxies classified as "Merger" using CAS.

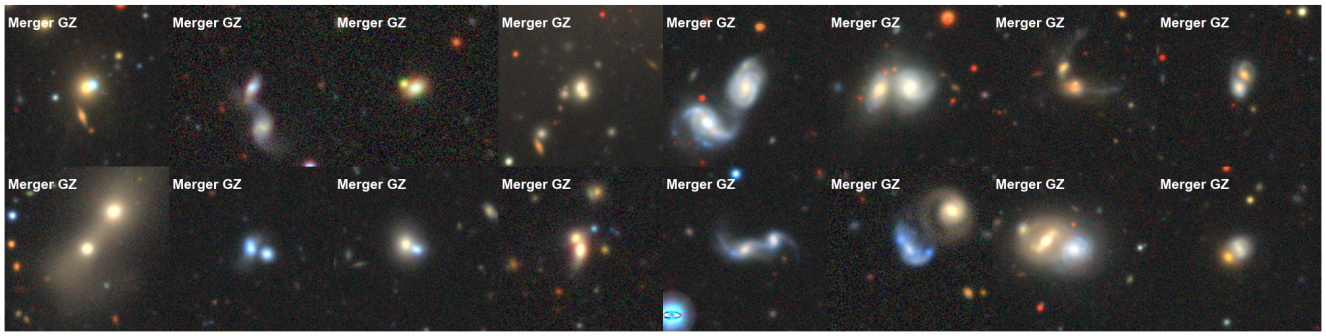

Figure 4.7: Random sample of galaxies classified as "Merger" using Galaxy Zoo (GZ).

In addition to the previously mentioned caveats related to the preprocessing of the FITS images before computing the CAS parameters, earlier studies suggest that the conditions $A > 0.35 \wedge A > S$ are not particularly efficient or accurate for identifying mergers. Conselice (2003) reported that only 50% of mergers were correctly identified using this method. Freeman et al. (2013) demonstrated that combining the Asymmetry parameter from CAS with MID statistics provides a more sensitive and effective approach for identifying disturbed morphologies such as mergers, because it detects noncontiguous groups of image pixels, their intensity values, and how much their distribution deviates from a smooth pattern.

In Figure 4.8 we present histograms of the vote fractions for "edge-on" and "merger" classifications of galaxies identified as such by CAS. For edge-on galaxies, we observe that nearly all galaxies classified as edge-on by CAS also have high vote fractions for this category in Galaxy Zoo, with only a few exceptions representing the contamination mentioned earlier. However, for mergers, most of the galaxies classified as such by CAS show low vote fractions for "merger" in Galaxy Zoo. Given that Galaxy Zoo classifies edge-on and merger galaxies reliably, we can use it as a reference to conclude that CAS performs well with edge-on galaxies but poorly with mergers.

We believe that Galaxy Zoo excels at identifying peculiar features in galaxies, as its volunteers can readily recognize them. This makes it particularly effective for detecting edge-on galaxies,

mergers, or other unique characteristics such as ring structures. In contrast, distinguishing between ellipticals, lenticulars, and disk galaxies can be more challenging.

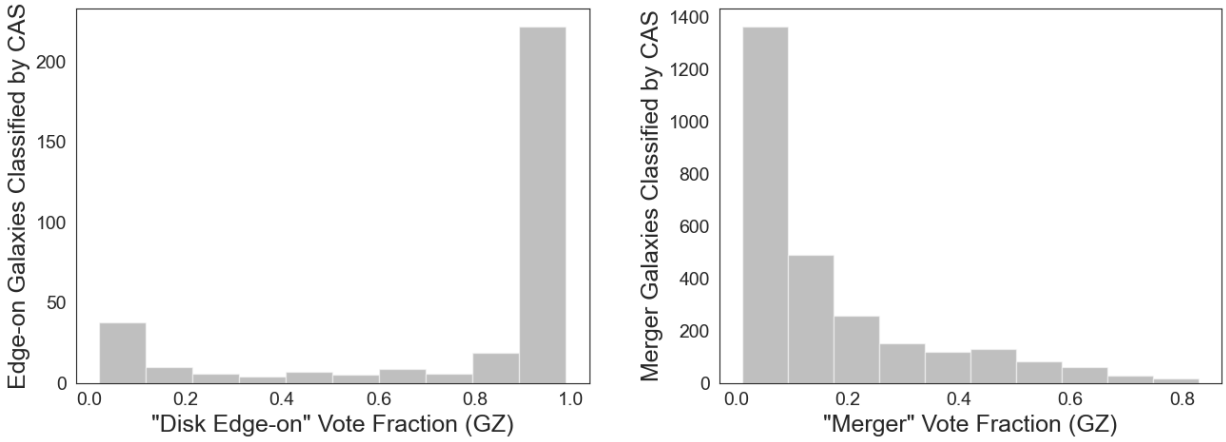

Figure 4.8: Histograms of the vote fractions for "Disk Edge-on" (left panel) and "Merger" (right panel) classifications of galaxies, classified respectively by CAS.

4.2 Morphology – Density Relation

We have established then that CAS is better for deriging general properties, while deep learning (GZ) performs better at identifying special cases such as mergers and edge-on galaxies. We reproduce the morphology-density relation to verify whether we observe the well-established trends and to further investigate its implications. Figure 4.9 shows the fractions of each of the six galaxy morphologies as a function of the measured galaxy densities, with a histogram above the plot, showing the number of galaxies within each bin of galaxy density. The error bars are calculated using the standard error for proportions, assuming a binomial distribution, with $z_{\alpha/2} = 1.96$, corresponding to a 95% confidence interval.

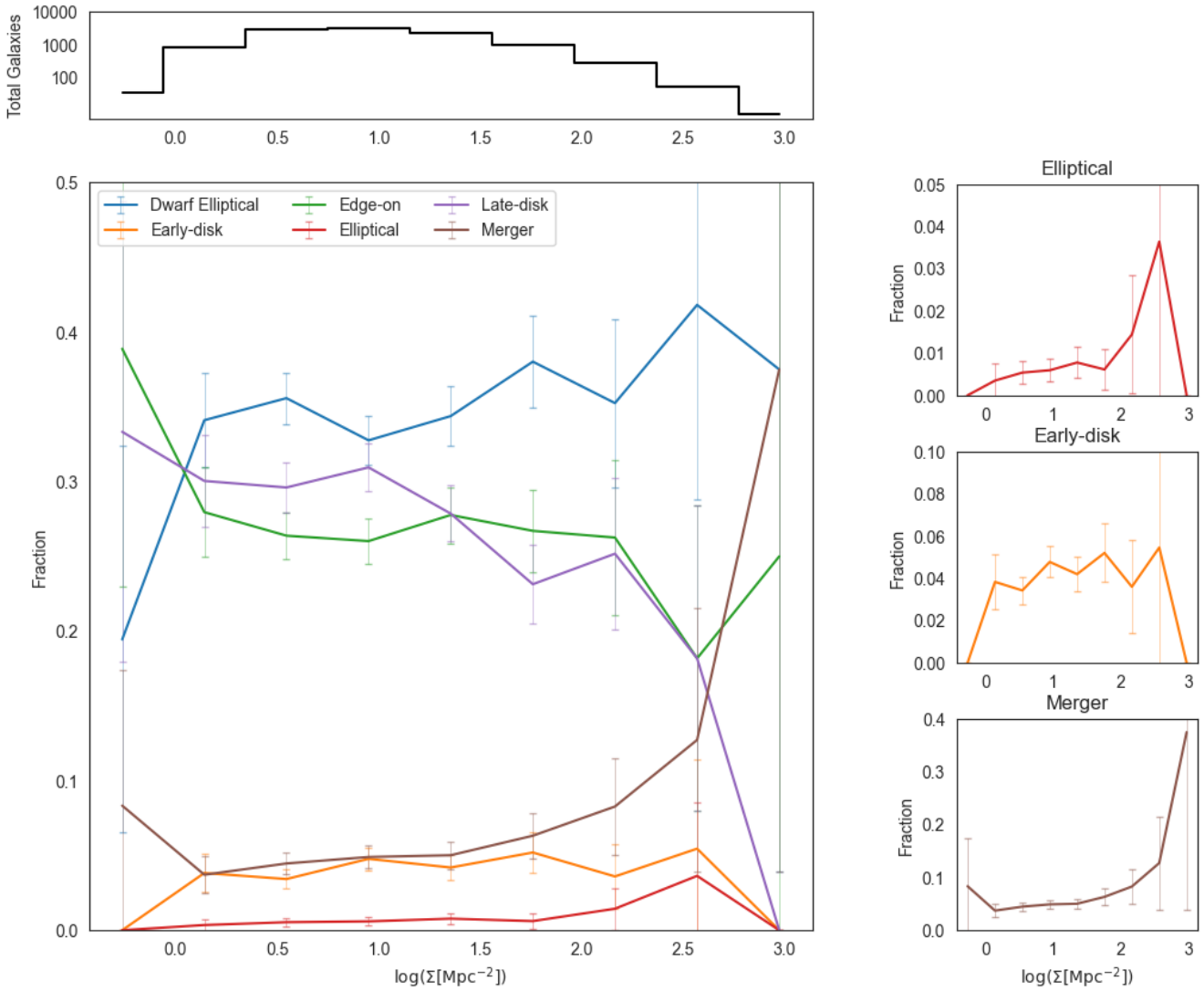

Figure 4.9: Morphology-density relation for dwarf elliptical (blue), early-disk (orange), edge-on (green), elliptical (red), late-disk (purple) and merger (brown) galaxies. The upper panel shows a histogram of the number of galaxies within each bin of galaxy density. The panels on the right highlight only the elliptical, early-disk, and merger fraction, to visualize it better.

As expected, the fraction of dwarf ellipticals increases with higher density. We observe a clear decline in the late-disk fraction as density increases. Early-disks increase in the lowest density bin, then remain relatively constant, with a decrease in the highest density bin. Giant ellipticals rise moderately, followed by a drastic increase, then a sharp decline in the highest density bin. Mergers stay steady initially, then increase with higher density. Edge-on disks show a decrease as density increases. Although the fraction of dwarf ellipticals increases, it does too rapidly, likely due to contamination from misclassified blue galaxies, as discussed in Section 4.1.1. To address this, we only considered dwarf ellipticals with a color index of $g - r > 0.6$, representing 75% of the

galaxies classified as dwarf ellipticals. In Figure 4.10, we show the morphology-density relation after applying this adjustment. The fraction of dwarf ellipticals now increases more gradually with increasing density, becoming the dominant fraction in the highest bins. It is important to note that the highest bin contains only 8 galaxies, so the fractions should be interpreted with caution.

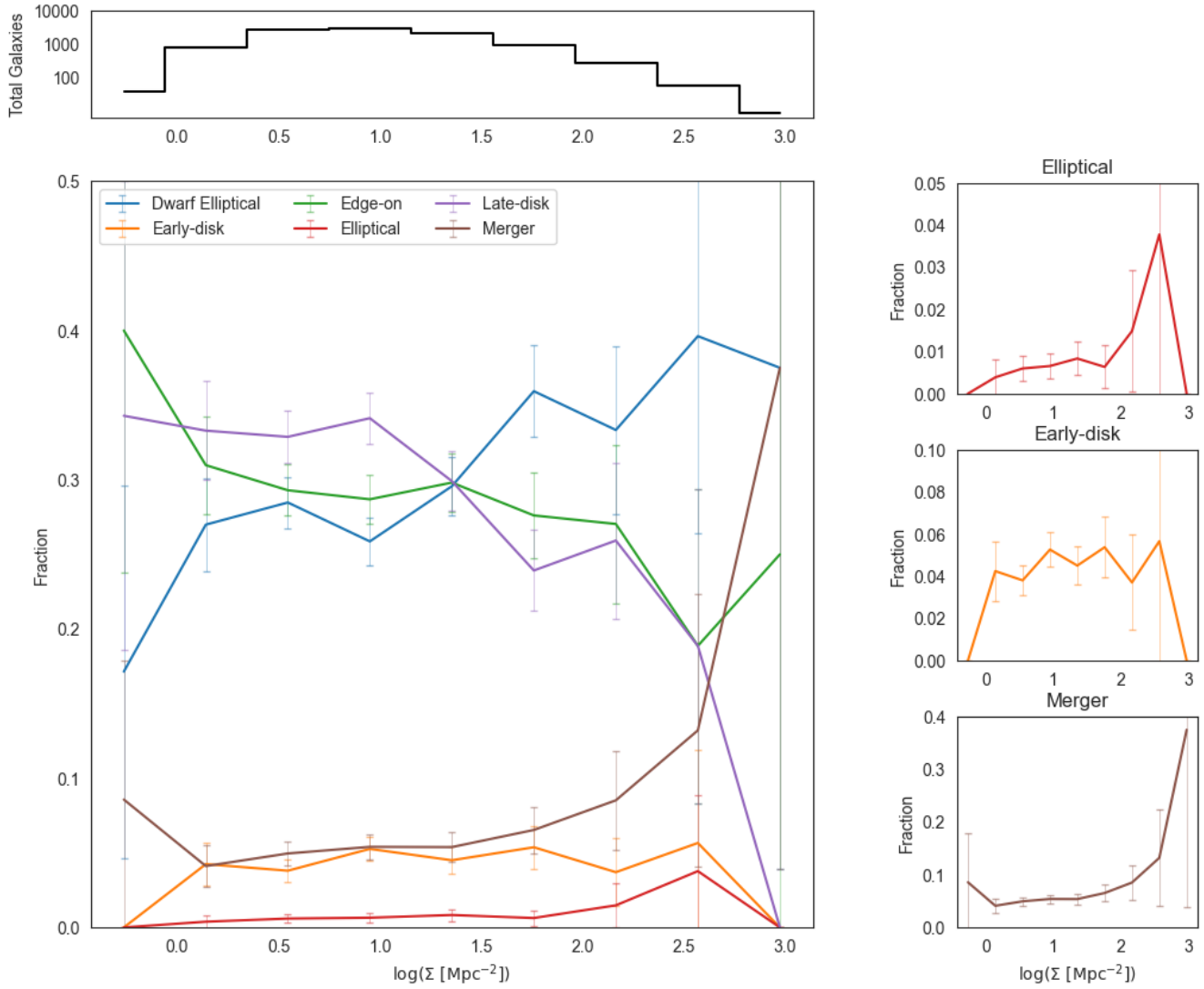

Figure 4.10: Morphology-density relation considering dwarf ellipticals with a color index $g-r > 0.6$.

The figure shows a change in the fraction of late disks at $\log(\Sigma) = 1$ where it suddenly decreases, while the fraction of dwarf ellipticals increases. This suggests a physical mechanism at work around this density. This result aligns with Goto et al. (2003), who observed a similar change at this density, but involving late disks and intermediate galaxies, and also identified it as the cluster infall region. Below this density, the fraction of late discs remains nearly constant, indicating the absence of a significant mechanism in this region. At the highest bins, the merger and elliptical

fractions increase, implying that density facilitates gravitational interactions and the evolution toward spheroidal galaxies. Furthermore, changes in the morphologies of ellipticals (both dwarf and giant) are observed before infall into the cluster, suggesting that local density may be more significant for elliptical galaxies compared to disk-type galaxies. These findings will be interpreted in Section 4.4.

4.3 Morphology – Radius Relation

Morphology is also known to correlate tightly with global environment , as parametrized by the cluster-centric distance, i.e, the radius from the center of the cluster. In Figure 4.10 we plot the morphology fractions against the cluster-centric distance in units of R_{200} (R/R_{200}). Same as before, the histogram shows the number of galaxies within each bin, the error bars are calculated using the standard error for proportions based on a binomial distribution, and the right panel highlights only the merger, early-disk and elliptical fraction, to visualize it better.

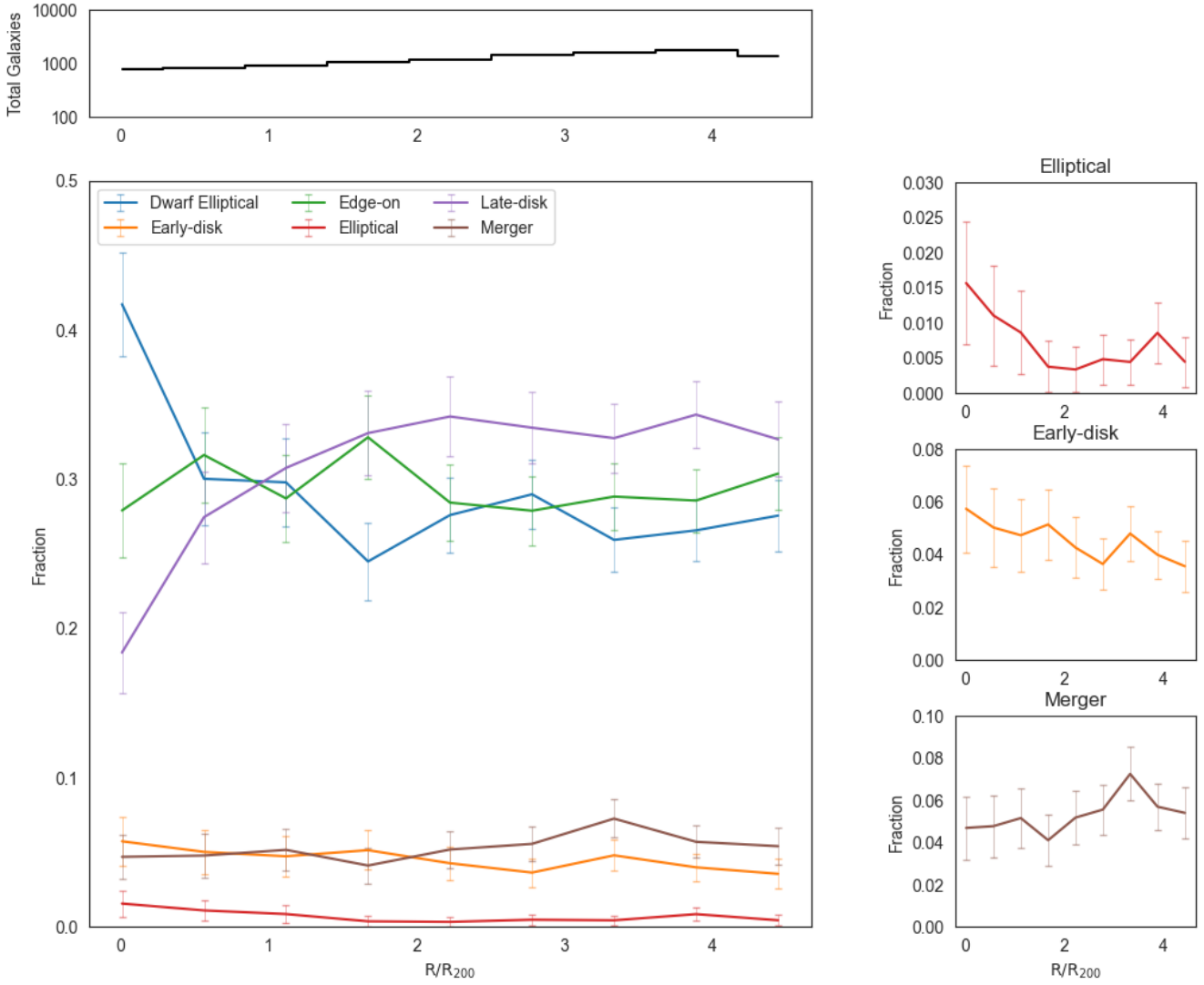

Figure 4.11: Morphology-radius relation for dwarf elliptical (blue), early-disk (orange), edge-on (green), elliptical (red), late-disk (purple) and merger (brown) galaxies. The upper panel shows a histogram of the number of galaxies within each bin of galaxy density. The panels on the right highlight only the elliptical, early-disk, and merger fraction, to visualize it better.

The fraction of dwarf and giant ellipticals decreases with increasing radius. Late-disks show an opposite trend, being more prominent in the outskirts of a cluster, while early-disks slightly decrease. Edge-on disks and mergers remain relatively constant across the radius range. Around $1R_{200}$, the fractions start becoming almost constant. This suggest that the mechanism responsible for the morphological changes stops affecting the galaxies at these radius. This is consistent with Goto et al. (2003). In this relation, we note that the mergers are not prominent in the center of the cluster, which is consistent with works that indicate mergers typically do not occur in this region due to the high relative velocity of galaxies, making close encounters less frequent (e.g. Mamon

(1992)). These findings will be interpreted in Section 4.4.

4.4 Density vs. Radius

We investigate the morphology-density relation for different regions of distance from the cluster center. For this, we follow a procedure similar to that of Goto et al. (2003), where the relation is divided at R_{200}. This is shown in Figure 4.12.

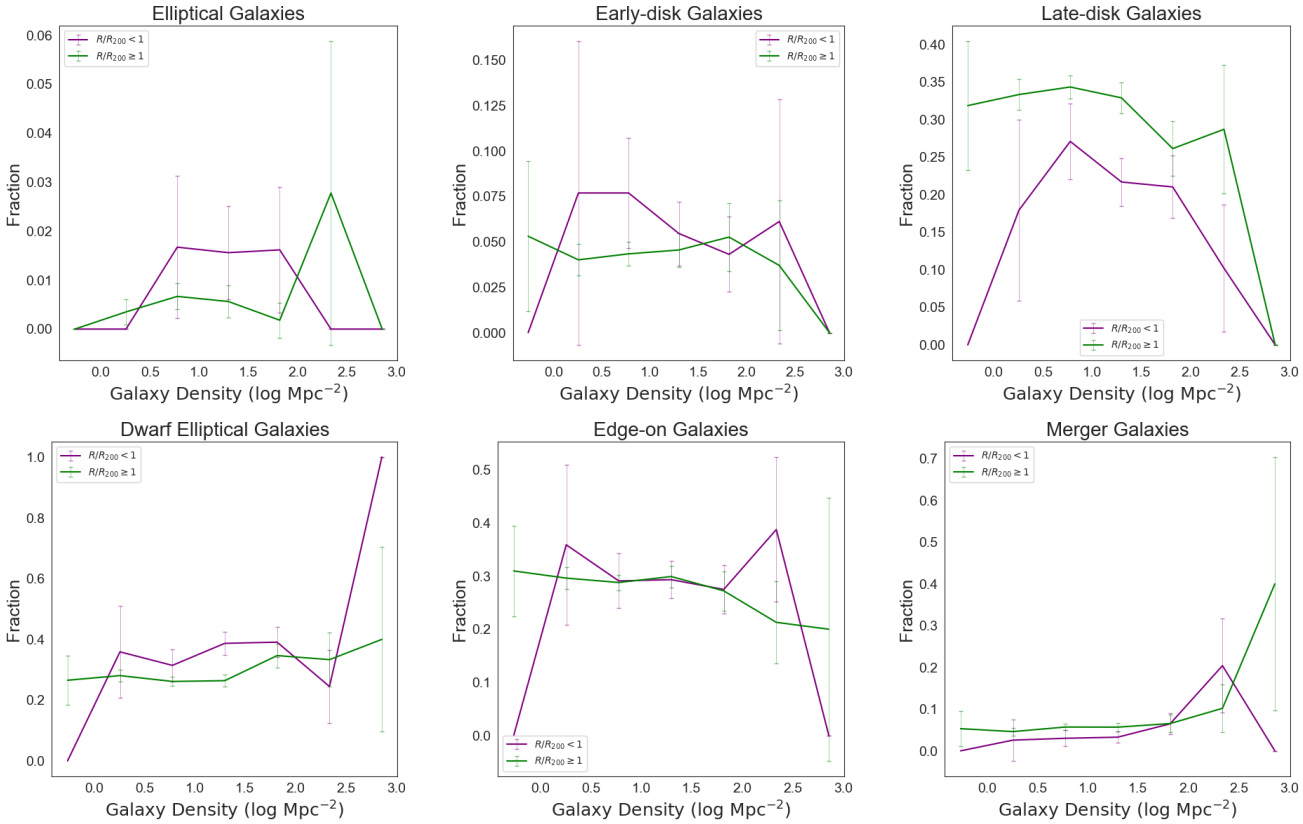

Figure 4.12: Morphology-density relation divided by R/R_{200} for each morphology type. The green line corresponds to $R/R_{200} \geq 1$, while the purple line corresponds to $R/R_{200} < 1$.

In the figure, elliptical galaxies are usually found within the virial radius; however, some high-density ellipticals are located outside this region. Dwarf elliptical galaxies are also observed within the virial radius, and in the highest density bin, all galaxies are confined to this region. Edge-on galaxies in intermediate-density environments are found both inside and outside the virial radius. Late-type disks predominantly lie outside the virial radius, with their fraction slightly decreasing in high-density regions. However, when considering only those within the virial radius, the fraction decreases significantly at higher densities[2]. Regarding early-type disks, a higher fraction is found

[2]We neglected the highest bin, as both fractions have 0 galaxies with a density within that bin.

within the virial radius. Finally, mergers are more likely to occur outside the virial radius, aligning with the idea that mergers are less frequent in the dense cores of clusters.

From the overall results of the morphology-density and morphology-radius relations, we observe that the fraction of elliptical galaxies increases with higher density and decreases with larger radii, as the cluster center is the densest region. However, they can also be found at high densities outside the core radius, suggesting that elliptical galaxies are primarily influenced by local density. This finding is consistent with Vulcani et al. (2023). For the case of late-type disks, their fraction increases with larger radii and decreases with high density. Outside the cluster radius, the fraction change slightly with higher density. However, when they infall into the cluster, near $1R_{200}$ and $\log(\Sigma) = 1$, they start decreasing suddenly. This suggests that they begin to undergo changes due to environmental effects, indicating that the global environment could be more important than local galaxy density. This also agrees with Vulcani et al. (2023). These findings align with the results of Domínguez et al. (2001): global mechanisms, such as the effects of the cluster environment, dominate in high-density regions within the virial radius, while local density prevails in the outskirts, where the cluster's overall influence is relatively minor compared to local effects.

A possible mechanism that could be changing the fraction of late-disk galaxies is ram pressure stripping, where cold gas is quickly stripped away due to the high pressure of the hot intracluster medium (Gunn and Gott, 1972), reducing the star formation rate. Another mechanism is strangulation, where star formation is truncated by the gradual removal of cold gas (Bekki et al., 2002). Both processes could lead to the evolution of galaxies into early-disk morphologies, which would explain why early-disk galaxies predominate within the virial radius in our sample. Over time, these galaxies could evolve into lenticular or intermediate-type galaxies. This would be an interesting topic for future study, adding this category to our analysis and including other properties, such as galaxy mass and size, as these are fundamental for observing the transition (Goto et al. (2003), Vulcani et al. (2023)). Mergers could account for the slight change in the fraction of spiral galaxies outside the virial radius as part of the preprocessing process. They might also be responsible for the formation of elliptical galaxies in higher-density regions beyond the virial radius. However, this mechanism alone cannot fully explain the presence of ellipticals within the virial radius, which may instead result from the evolutionary transformation of disk galaxies.

Chapter 5

Conclusions

In this study, we utilized publicly available Galaxy Zoo DESI classifications, which combine citizen science and deep learning, and CAS measurements to classify galaxies in the CHANCES target selection catalog. This catalog contains photometric members of over 50 galaxy clusters, extending out to $5R_{200}$. The first goal was to evaluate which classification method performs better for different morphological types. After classifying the galaxies, we analyzed the morphology-density and morphology-radius relations.

Regarding the classification methods:

1. We used a threshold of 0.5 vote fraction to classify galaxies using Galaxy Zoo, successfully classifying 43.885 galaxies. Many galaxies in the CHANCES catalog were not part of GZ due to cases of shredding or failure to meet the filters applied by GZ.

2. Using `statmorph`, we calculated the CAS parameters and classified galaxies based on predefined parameter ranges for each morphology. This approach successfully classified only 11.321 galaxies. Many galaxies could not be classified due to strict parameter boundaries, and poor measurement quality caused by contaminating objects in the FITS files or the use of FITS with inappropriate pixel scales for the angular size of the galaxies.

3. CAS performed better in classifying elliptical galaxies, as it provided more accurate classifications for these types of galaxies. Galaxy Zoo tended to classify too many low-resolution blue galaxies as "smooth," leading to contamination in the early-type galaxy category.

4. CAS was more effective in classifying disk galaxies, as it reduced contamination from redder galaxies and allowed better differentiation between early-disk and late-disk morphologies.

5. Galaxy Zoo excelled at identifying mergers and edge-on disk galaxies. These morphologies have distinct appearances that are easily recognized by citizen scientists and thus captured effectively by the deep learning-trained model.

6. Although CAS generally classified edge-on disk galaxies well, it sometimes misclassified face-on galaxies as edge-on. Additionally, CAS often incorrectly identified many galaxies as mergers. For merger classification, it is recommended to combine the asymmetry parameter with other non-parametric methods, such as MID statistics, for better accuracy.

From the study of the morphology-density and morphology-radius relations, we found that:

1. The fraction of elliptical galaxies increases with higher densities and shorter radii. They are also found in high-density regions outside the cluster radius, suggesting that their morphology is primarily influenced by local density.

2. Mergers are more likely to occur outside the virial radius and at higher densities. This mechanism alone cannot explain the ellipticals found within the virial radius.

3. The fraction of late-type disk galaxies increases with larger radii and decreases with higher densities. Outside the radius of the cluster, the local density is more important. As they infall into the cluster, environmental effects dominate. Mechanisms like ram pressure stripping and strangulation may be inducing the morphological transformations inside the cluster, and mergers outside the cluster.

Future studies will focus on improving galaxy classifications by incorporating the lenticular morphology, which will enable us to better explore the evolutionary paths of galaxies. This could be complemented by integrating key properties such as galaxy mass and size, which are essential for understanding these transitions, as highlighted by previous research (Goto et al. (2003), Vulcani et al. (2023)). Other important improvements involve using FITS images with the right scale and removing contaminating objects to make the CAS measurements more accurate, and implementing a supervised machine learning model to classify a larger number of galaxies. For galaxies that do not match the Galaxy Zoo catalog, we could use transfer learning with the deep learning model used by GZ, Zoobot, which is publicly available. Additionally, future work should include the computation of completeness and contamination for each morphological type to ensure more reliable results. These advancements will refine our understanding of the environmental mechanisms and evolutionary processes that shape galaxy morphologies.

Bibliography

Bekki, K., Couch, W. J., and Shioya, Y. (2002). Passive spiral formation from halo gas starvation: Gradual transformation into s0s. *The Astrophysical Journal*, 577(2):651.

Bond, J. R., Kofman, L., and Pogosyan, D. (1996). How filaments of galaxies are woven into the cosmic web. , 380(6575):603–606.

Bradley, L., Sipőcz, B., Robitaille, T., Tollerud, E., Vinícius, Z., Deil, C., Barbary, K., Wilson, T. J., Busko, I., Donath, A., Günther, H. M., Cara, M., Lim, P. L., Meßlinger, S., Conseil, S., Burnett, Z., Bostroem, A., Droettboom, M., Bray, E. M., Bratholm, L. A., Ginsburg, A., Jamieson, W., Barentsen, G., Craig, M., Morris, B. M., Perrin, M., Rathi, S., Pascual, S., and Georgiev, I. Y. (2024). astropy/photutils: 2.0.2.

Byrd, G. and Valtonen, M. (1990). Tidal Generation of Active Spirals and S0 Galaxies by Rich Clusters. , 350:89.

Cabrera-Vives, G., Miller, C. J., and Schneider, J. (2018). Systematic labeling bias in galaxy morphologies. *The Astronomical Journal*, 156(6):284.

Conselice, C. J. (2003). The relationship between stellar light distributions of galaxies and their formation histories. *The Astrophysical Journal Supplement Series*, 147(1):1.

Domínguez, M., Muriel, H., and Lambas, D. G. (2001). Galaxy morphological segregation in clusters: Local versus global conditions. *The Astronomical Journal*, 121(3):1266–1274.

Dressler, A. (1980). Galaxy morphology in rich clusters: implications for the formation and evolution of galaxies. , 236:351–365.

Freeman, P. E., Izbicki, R., Lee, A. B., Newman, J. A., Conselice, C. J., Koekemoer, A. M., Lotz, J. M., and Mozena, M. (2013). New image statistics for detecting disturbed galaxy morphologies at high redshift. , 434(1):282–295.

Goto, T., Yamauchi, C., Fujita, Y., Okamura, S., Sekiguchi, M., Smail, I., Bernardi, M., and Gomez, P. L. (2003). The morphology-density relation in the Sloan Digital Sky Survey. , 346(2):601–614.

Gunn, J. E. and Gott, J. Richard, I. (1972). On the Infall of Matter Into Clusters of Galaxies and Some Effects on Their Evolution. , 176:1.

Hubble, E. P. (1926). Extragalactic nebulae. , 64:321–369.

Kodama, T. and Bower, R. G. (2001). Reconstructing the history of star formation in rich cluster cores. *Monthly Notices of the Royal Astronomical Society*, 321(1):18–36.

Lotz, J. M., Primack, J., and Madau, P. (2004). A New Nonparametric Approach to Galaxy Morphological Classification. , 128(1):163–182.

Mamon, G. A. (1992). Are Cluster Ellipticals the Products of Mergers? , 401:L3.

Medina-Rosales, E., Cabrera-Vives, G., and Miller, C. J. (2024). Mitigating bias in deep learning: training unbiased models on biased data for the morphological classification of galaxies. *Monthly Notices of the Royal Astronomical Society*, 531(1):52–60.

Moore, B., Katz, N., Lake, G., Dressler, A., and Oemler, A. (1996). Galaxy harassment and the evolution of clusters of galaxies. , 379(6566):613–616.

Rodriguez-Gomez, V., Snyder, G. F., Lotz, J. M., Nelson, D., Pillepich, A., Springel, V., Genel, S., Weinberger, R., Tacchella, S., Pakmor, R., Torrey, P., Marinacci, F., Vogelsberger, M., Hernquist, L., and Thilker, D. A. (2019). The optical morphologies of galaxies in the IllustrisTNG simulation: a comparison to Pan-STARRS observations. , 483(3):4140–4159.

Sérsic, J. L. (1963). Influence of the atmospheric and instrumental dispersion on the brightness distribution in a galaxy. *Boletin de la Asociacion Argentina de Astronomia La Plata Argentina*, 6:41–43.

Sifón, C., Finoguenov, A., Haines, C. P., Jaffé, Y., Amrutha, B. M., Demarco, R., Lima, E. V. R., Lima-Dias, C., Méndez-Hernández, H., Merluzzi, P., Monachesi, A., Teixeira, G. S. M., Tejos, N., Araya-Araya, P., Argudo-Fernández, M., Baier-Soto, R., Bilton, L. E., Bom, C. R., Calderón, J. P., Cassarà, L. P., Comparat, J., Courtois, H. M., D'Ago, G., Dupuy, A., Fritz, A., Haack, R. F., Herpich, F. R., Ibar, E., Kuchner, U., Lopes, A. R., Lopez, S., Lösch, E., McGee, S., de Oliveira, C. M., Morelli, L., Moretti, A., Pallero, D., Piraino-Cerda, F., Pompei, E., Rescigno, U., Smith, R., Castelli, A. V. S., Jr, L. S., and Tempel, E. (2024). Chances, the chilean cluster galaxy evolution survey: selection and initial characterization of clusters and superclusters.

Vavilova, I. B., Dobrycheva, D. V., Vasylenko, M. Yu., Elyiv, A. A., Melnyk, O. V., and Khramtsov, V. (2021). Machine learning technique for morphological classification of galaxies from the sdss - i. photometry-based approach. *AA*, 648:A122.

Vulcani, B., Poggianti, B. M., Gullieuszik, M., Moretti, A., Fritz, J., Bettoni, D., Facciolli, B., Fasano, G., and Omizzolo, A. (2023). Clustercentric distance or local density? it depends on galaxy morphology. *The Astrophysical Journal*, 949(2):73.

Walmsley, M., Géron, T., Kruk, S., Scaife, A. M. M., Lintott, C., Masters, K. L., Dawson, J. M., Dickinson, H., Fortson, L., Garland, I. L., Mantha, K., O'Ryan, D., Popp, J., Simmons, B., Baeten, E. M., and Macmillan, C. (2023). Galaxy Zoo DESI: Detailed morphology measurements for 8.7M galaxies in the DESI Legacy Imaging Surveys. , 526(3):4768–4786.

Whitmore, B. C., Gilmore, D. M., and Jones, C. (1993). What Determines the Morphological Fractions in Clusters of Galaxies? , 407:489.

Appendix A

Mosaics

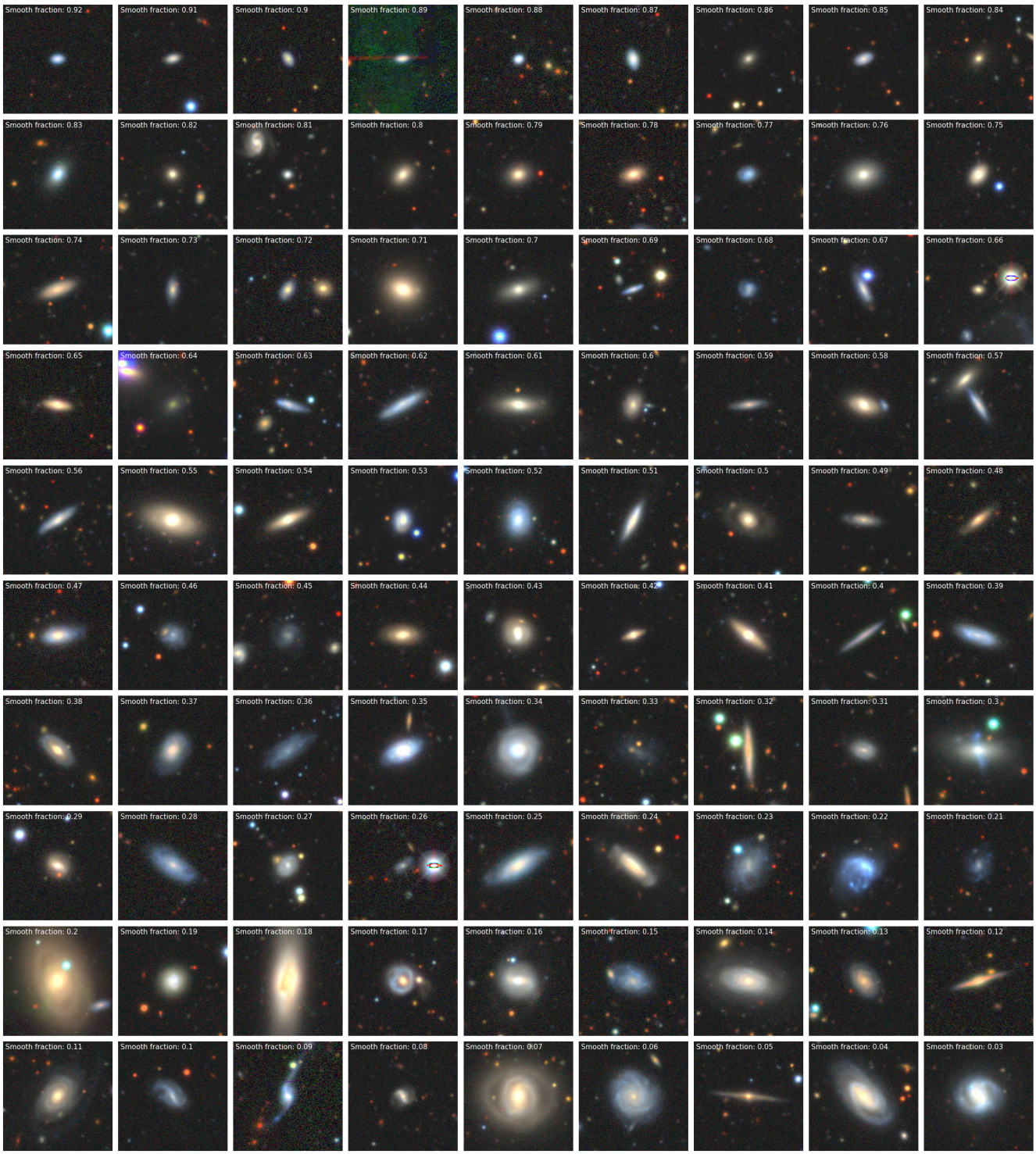

Figure A.1: Mosaic displaying images of a random galaxy for each vote fraction associated with the answer "Smooth". Each image includes the corresponding vote fraction value.

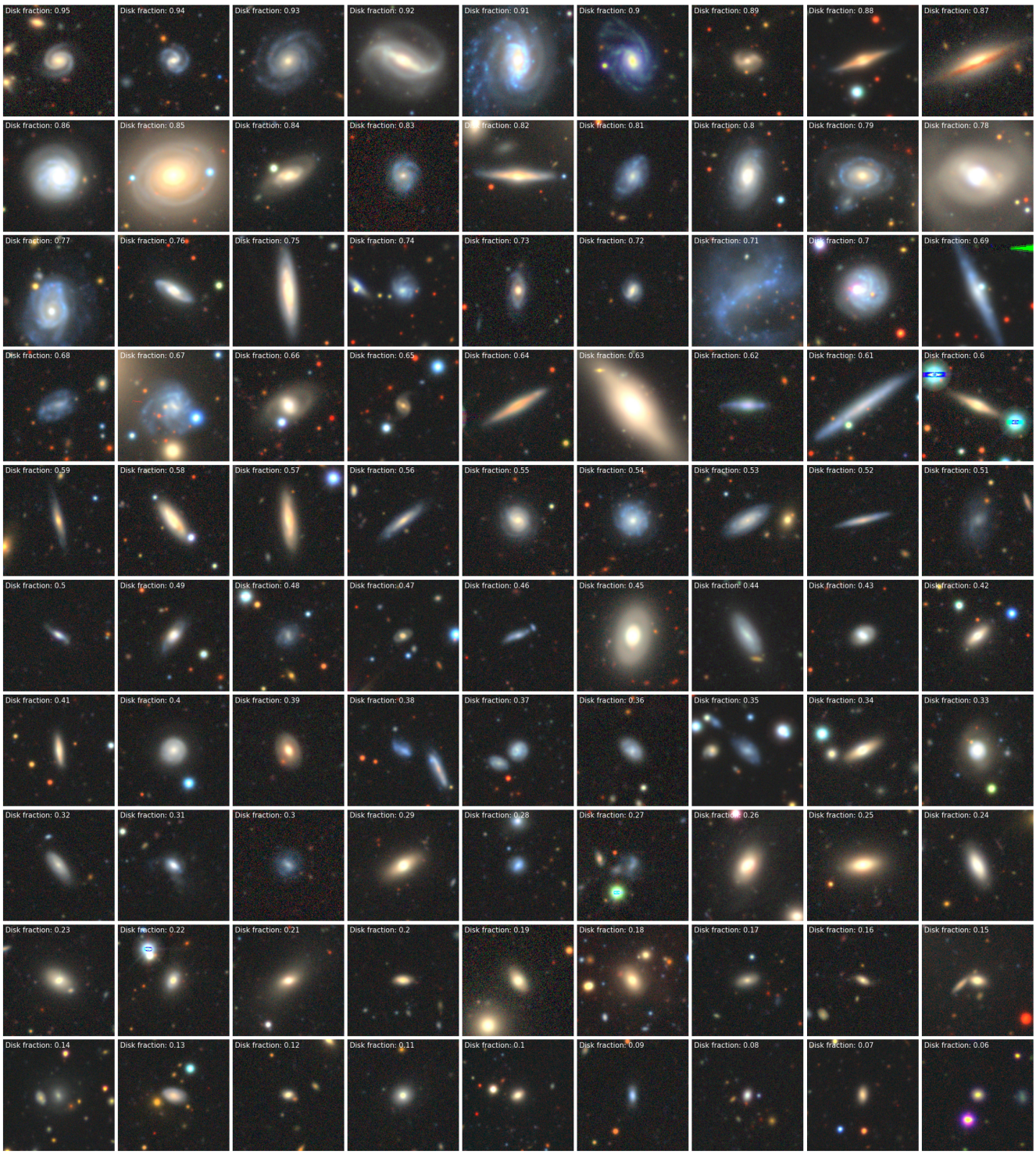

Figure A.2: Mosaic displaying images of a random galaxy for each vote fraction associated with the answer "Features or disk". Each image includes the corresponding vote fraction value.

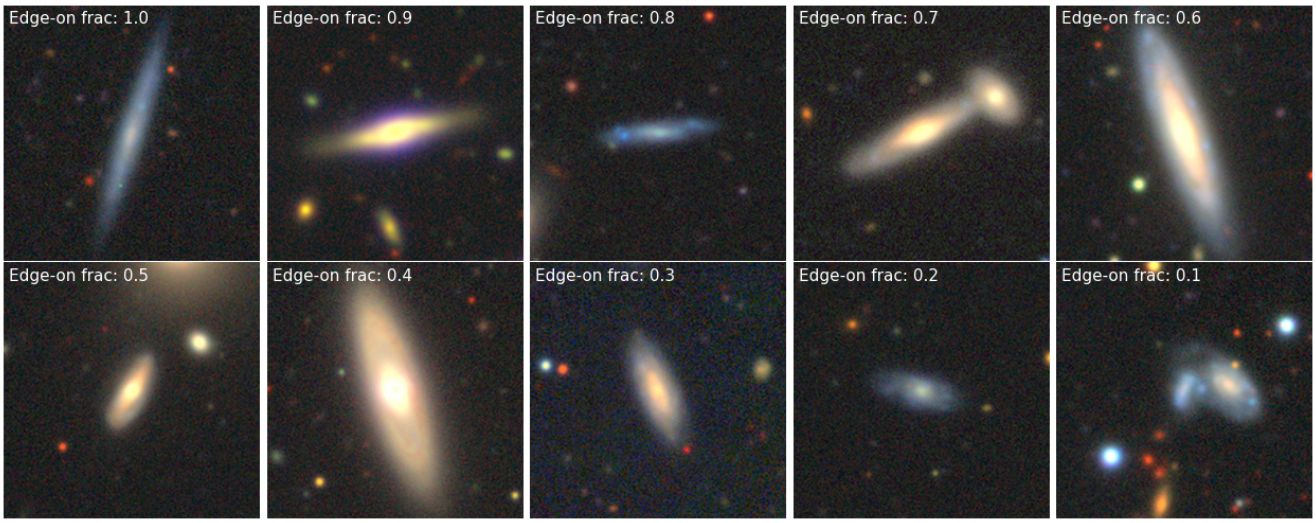

Figure A.3: Mosaic displaying images of a random galaxy for each vote fraction associated with the answer "Edge-on disk". Each image includes the corresponding vote fraction value.

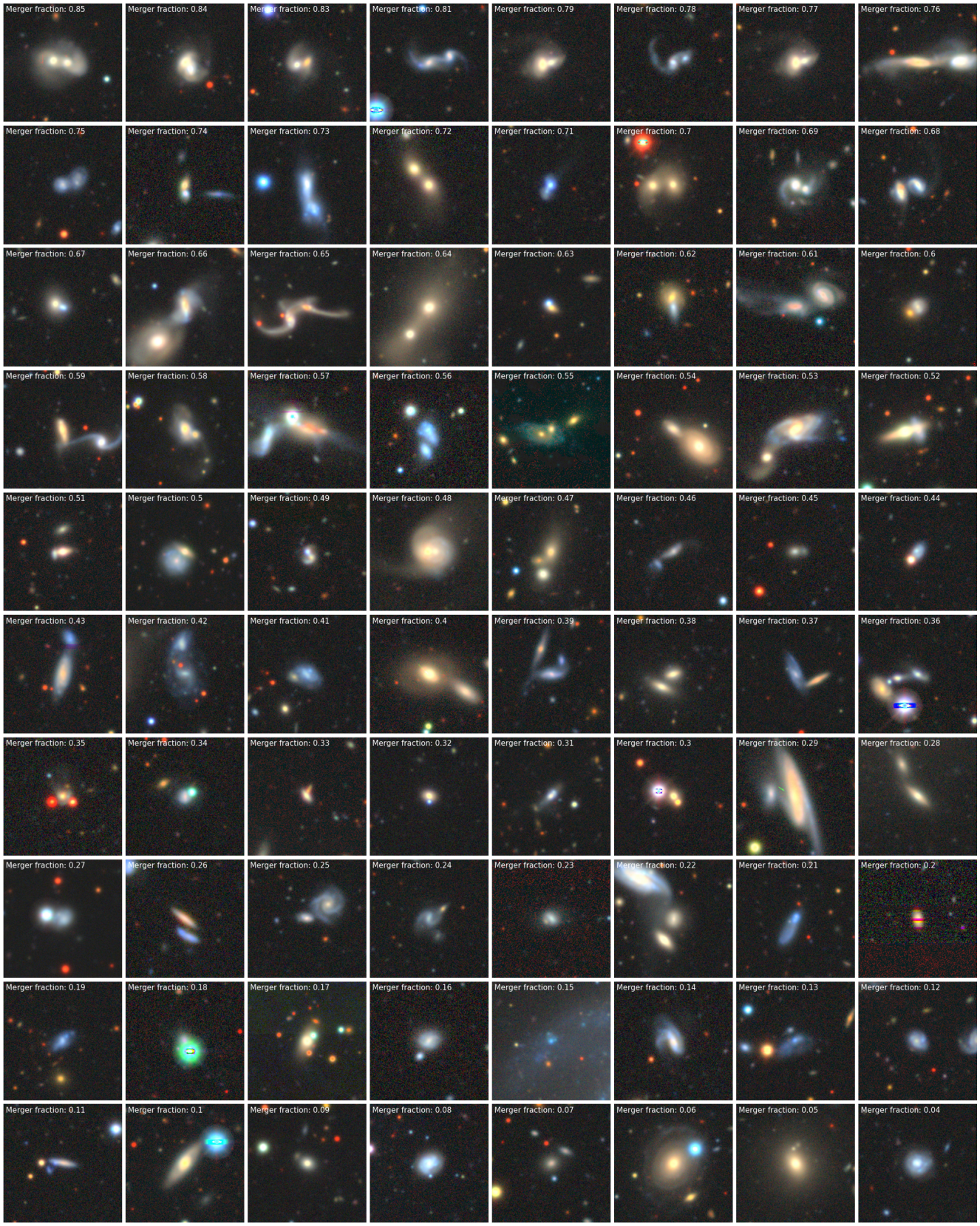

Figure A.4: Mosaic displaying images of a random galaxy for each vote fraction associated with the answer "Merger". Each image includes the corresponding vote fraction value.